Magnetic catalysis in hot and dense quark matter and quantum fluctuations

Kenji Fukushima
Department of Physics, Keio University, Kanagawa 223-8522, Japan

Jan M. Pawlowski
Institut für Theoretische Physik, Universität Heidelberg, Philosophenweg 16, 69120 Heidelberg, Germany

We analyze chiral symmetry breaking in quark matter in an external magnetic field at zero and finite temperature and quark chemical potential. We first give a brief overview of analytic results within the mean-field approximation. There the critical temperature for chiral restoration is increased by the magnetic field effect. Then we investigate the effects of matter and quantum fluctuations on the Magnetic Catalysis. More specifically, we compute the critical coupling as a function of the magnetic field and the temperature for zero and finite quark chemical potential in the presence of quantum fluctuations. As soon as a non-zero temperature and/or density is turned on, long-range correlations are screened and the critical coupling is no longer vanishing. We extend our dynamical results beyond the leading-order bubble resummation which results in a non-local four-Fermi coupling. This includes in-medium meson effects on the more quantitative level.

PACS numbers: 11.30.Rd, 11.10.Hi, 11.10.Wx, 21.65.Qr, 12.38.-t

I. INTRODUCTION

The state of matter in a strong magnetic field $\boldsymbol{B}$ still poses interesting theoretical as well as experimental challenges. In the Landau quantization approach to these situations the energy dispersion relation of charged particles is quantized along the directions perpendicular to $\boldsymbol{B}$. There are a countless number of interesting phenomena related to the Landau quantization such as the Quantum Hall Effect in condensed matter physics [1], the Chiral Magnetic Effect in the relativistic heavy-ion collision [2, 3] and related phenomena [4], the primordial magnetic field in cosmological phase transitions [5]. In the present work we concentrate on the Magnetic Catalysis, [6], in the context of hot and dense quark matter.

In relativistic heavy-ion collisions the state of matter undergoes a phase transition or cross-over from the quark-gluon plasma of strongly interacting quark and gluon (quasi)-particles to the hadronic phase with chiral symmetry breaking and confinement. Recently, $\boldsymbol{B}$-induced phenomena within these phase transitions are attracting more and more theoretical and experimental interest. This is motivated by the recognition of the presence of extraordinary strong $\boldsymbol{B}$ in the early stage of non-central collisions [2]. The specific importance of $\boldsymbol{B}$ over the electric field $\boldsymbol{E}$ is that $\boldsymbol{B}$ is not screened by charged particles unlike $\boldsymbol{E}$. The strength of $\boldsymbol{B}$ can get as large as $|e\boldsymbol{B}| \sim \Lambda_{\rm QCD}^2$, while its life time is also characterized by $\sim \Lambda_{\rm QCD}^{-1}$ and thus is very small [7]. Nevertheless, it is conceivable to anticipate observable $\boldsymbol{B}$ effects in the distribution of produced particles [8] since the production process occurs within the time scale of the strong interaction or even faster.

By now model analyses according to the hydrodynamic description of the heavy-ion collision suggest that the thermalization is rapidly achieved before $\tau \sim 0.6$ fm/c [9]. Because $\boldsymbol{B}$ decays not exponentially but by the power as a function of time, the magnetic field strength is still comparable to the QCD scale when the system gets thermalized. Consequently it is a very interesting question how the QCD phase transition is modified by the strong $\boldsymbol{B}$ effects.

Within the framework of effective model studies it was found that the chiral phase transition is significantly delayed (i.e. the critical temperature is increased) by $\boldsymbol{B}$, while the deconfinement transition or the Polyakov loop behavior is hardly affected [10–12]. This latter result on deconfinement, however, turned out to be inconsistent with the lattice-QCD simulation [13, 14]. Even though there are some attempts to account for the significant modification in the Polyakov loop behavior by introducing extra couplings [15, 16], the microscopic details about the coupling between the gluonic dynamics and the external magnetic field are not fully understood yet. The missing coupling is possibly attributed to screening by polarization effects, which has the same origin as the failure of chiral model approaches to baryon-rich matter [17, 18]. There it has been shown within QCD computations that the polarization effects have a considerable impact on the location of the confinement-deconfinement phase transition; see Refs. [19, 20]. Indeed, in Ref. [21] it has been shown that the interplay between strong electromagnetic and chromo-electric and chromo-magnetic fields gives rise to polarization effects that catalyze the deconfinement phase transition. This already hints at the similarity between large-$\boldsymbol{B}$ effect and high-$\mu_{\rm q}$ effect which may give a clue for attacking the problems at high density, as emphasized in Ref. [22].

In contrast to deconfinement, the $\boldsymbol{B}$ effects on the chiral phase transition is naturally understood from the qualitative effects implied by the so-called Magnetic Catalysis [6] which was first discovered in fermionic theory with four-Fermi interaction, and later the argument was extended to QED as well [23]. When $\boldsymbol{B}$ is sufficiently strong, the magnetic field plays a role as the catalysis

that induces a finite chiral condensate $\langle\bar{\psi}\psi\rangle$. Since chiral symmetry breaking is enhanced by $\boldsymbol{B}$, it is natural to anticipate a higher critical temperature for chiral restoration than in the case with vanishing $\boldsymbol{B}$. This expectation was indeed confirmed in recent model studies [24] and indeed was observed already before the discovery of the Magnetic Catalysis [25]. In recent lattice-QCD simulation [14] it was found that $T_{\rm c}$ significantly decreases for larger $\boldsymbol{B}$, which can be interpreted as a result of the entanglement with the Polyakov loop that is affected by the magnetic screening [26]. Such screening has been discussed in Ref. [21] for the gluonic potential. In this sense, as long as only the chiral sector is concerned, the enhancement of the chiral condensate by $\boldsymbol{B}$ is not contradictory to Ref. [14]. Also, regarding another possibility of the inverse Magnetic Catalysis at finite density, see Ref. [27].

The purpose of this paper is to study the $\boldsymbol{B}$ effects on the chiral phase transition including quantum fluctuations. These effects of quantum fluctuations are quite naturally included with renormalization group (RG) flows which also shed light on the physics mechanisms at work (see Refs. [12, 28, 29] for related works). We calculate the β-function for the four-Fermi coupling constant λ_k as a function of an IR cutoff scale k. At large cutoff scales k implying large energies we are in the chirally symmetric phase with vanishing chiral condensate $\langle\bar{\psi}\psi\rangle = 0$. Chiral symmetry breaking is signaled by a singularity in the four-Fermi coupling related to the appearance of massless pion (and sigma) propagation in the intermediate state of the four-point vertex at vanishing momenta. Hence by decreasing the cutoff scale k the RG-flow of λ_k hits this singularity at some point (see Ref. [30] for a recent comprehensive review). In this paper we adopt a chiral model for simplicity. In this way we can get a simple formula for the critical surface in space spanned by the four-Fermi coupling λ_k, the temperature T, and the quark chemical potential $\mu_{\rm q}$ with and without a constant magnetic field $\boldsymbol{B}$. The extension or embedding of the model results obtained here within the RG approach to QCD is straightforward; see Refs. [20, 30].

This paper is organized as follows. We first present a brief overview of the mean-field results for the critical coupling in Sec. II. This part is used for introducing our notation and it also has the benefit of allowing an easy comparison of the mean-field arguments and results with those of the RG analysis in Sec. III. Finally we extend the RG analysis by including meson effects beyond the leading-order bubble resummation to the four-Fermi coupling in Sec. IV. As we shall see in Sec. III there are three different kinds of Feynman diagrams that contribute to the β-function of λ_k. Two of them tend to break chiral symmetry and are genuinely fermionic in nature. The last one forms a box-type diagram that favors chiral restoration and this box diagram contains intermediate meson states with finite momentum insertion. This additional resummation establishes the well-known effect that fermionic fluctuations tend to break chiral symmetry whereas mesonic ones tend to restore it. We find that the box diagram has only a minor effect on the Magnetic Catalysis when $\boldsymbol{B}$ is large. Section V is devoted to the conclusion and outlook.

II. OVERVIEW OF THE MEAN-FIELD CALCULATION

Here we recall spontaneous chiral symmetry breaking on the mean-field level with and without magnetic field. We intend to capture the generic feature of chiral symmetry breaking in an effective description. Integrating-out the gluons in QCD as well as the quark fluctuations with momenta larger than a ultraviolet (UV) cutoff scale Λ would lead to a chiral effective theory formulated in terms of quarks with all kinds of interaction vertices; see e.g. Refs. [19, 20, 31, 32]. Among these vertices only the point-like four-point interaction is retained for simplicity, which defines the Nambu–Jona-Lasinio (NJL) model. In what follows we consider hot and dense quark matter with three colors, $N_{\rm c} = 3$, and two massless flavors, $N_{\rm f} = 2$. Then the Lagrangian density at the UV scale Λ reads

$$\mathcal{L}_\Lambda = \bar{\psi}\,\mathrm{i}\partial\!\!\!/\psi + \frac{1}{2}\,\bar{\psi}_i^{a\alpha}\psi_j^{b\alpha}\;\Gamma_{\Lambda}{}_{ijlm}^{abcd}\;\bar{\psi}_l^{c\beta}\psi_m^{d\beta}\;, \qquad (1)$$

where α and β run in color space, a, b, c, d in flavor space, and i, j, l, m refer to the Dirac indices. We take the sum over repeated indices as usual. For the concrete form of $\Gamma_{\Lambda}{}_{ijlm}^{abcd}$ we assume an equal mixing of the $\mathrm{U(1)_A}$-symmetric and $\mathrm{U(1)_A}$-breaking terms so that the iso-scalar pseudo-scalar particle (η_0) and the iso-vector scalar particles ($\vec{a_0}$) decouple from low-lying spectra. The remaining interaction vertices contain the iso-scalar scalar channel (σ) and the iso-vector pseudo-scalar ($\vec{\pi}$) channels only,

$$\Gamma_{\Lambda}{}_{ijlm}^{abcd} = \lambda_\Lambda\big[\delta_{ij}\delta_{lm}\delta^{ab}\delta^{cd} + (\mathrm{i}\gamma_5)_{ij}(\mathrm{i}\gamma_5)_{lm}(\tau^n)^{ab}(\tau^n)^{cd}\big]\,, \qquad (2)$$

where τ^n's are the Pauli matrices in flavor space and n runs from 1 to $N_{\rm f}^2 - 1$ corresponding to pion degrees of freedom.

We close with the remark that the Lagrangian (2) was introduced as already comprising all quantum effects of quark fluctuations with momenta larger than the cutoff scale as well as all gluonic fluctuations. This implies that (2) should have included terms depending on Λ as well as the physical mass scales of QCD ($\Lambda_{\rm QCD}, m_{\rm quark}$) such that if introducing the missing quantum fluctuations of the quarks, the result is Λ-independent. This necessity is avoided by assuming Λ to be such that these terms are minimized. This gives a physical meaning to Λ and it is rather $\Lambda_{\rm QCD}$ up to a constant than a UV cutoff scale.

A. Gap equation and the critical coupling constant

In the mean-field approximation the four-Fermi interaction is decomposed into the mean-field $\langle\bar{\psi}\psi\rangle$ and the fluctuations about it. We pick up only the contribution from the non-crossing color structure, $\langle\bar{\psi}^\alpha\psi^\alpha\rangle\,\bar{\psi}^\beta\psi^\beta$, but simply neglect the crossing one like $\langle\bar{\psi}^\alpha\psi^\beta\rangle\,\bar{\psi}^\beta\psi^\alpha$. Such a treatment is justified in the large-N_c limit in which the mean-field approximation also becomes exact. The constituent quark mass, $M=-\lambda_\Lambda\langle\bar{\psi}\psi\rangle$, appears as a result of the spontaneous chiral symmetry breaking, and the mean-field Lagrangian density reads

$$\begin{aligned}\mathcal{L}_\mathrm{MF} &= \bar{\psi}\,\mathrm{i}\partial\!\!\!/\psi + \lambda_\Lambda\langle\bar{\psi}\psi\rangle\,\bar{\psi}\psi - \frac{\lambda_\Lambda}{2}\langle\bar{\psi}\psi\rangle^2 \\ &= \bar{\psi}(\,\mathrm{i}\partial\!\!\!/ - M)\psi - \frac{M^2}{2\lambda_\Lambda} \end{aligned} \tag{3}$$

in the chiral limit. The Lagrangian density (3) bilinear in the quark fields, and hence the path integral quantization is done by a Gaussian integration. The resulting thermodynamic potential is a function of M and is given by

$$\begin{aligned}\beta\Omega/V = -2N_\mathrm{c}N_\mathrm{f}\int_{p^2\le\Lambda^2}\frac{\mathrm{d}^3p}{(2\pi)^3}\Big\{\omega + T\ln\big[1+\mathrm{e}^{-\beta(\omega-\mu_\mathrm{q})}\big] \\ + T\ln\big[1+\mathrm{e}^{-\beta(\omega+\mu_\mathrm{q})}\big]\Big\} + \frac{M^2}{2\lambda_\Lambda}\end{aligned} \tag{4}$$

with the quasi-particle energy dispersion relation, $\omega=\sqrt{p^2+M^2}$. The momentum integral is cut at the cutoff scale as the mean field Lagrangian (3) supposedly arising from integrating-out the quarks with momenta larger than the cutoff scale, $p^2>\Lambda^2$. The overall constant 2 comes from the spin degeneracy. For the moment we restrict ourselves to vanishing temperature and density; $T=\mu_\mathrm{q}=0$. Later we extend the analysis to include thermal and medium effects. In this simple setup the momentum integral in Eq. (4) can only lead to a function of $\xi=M/\Lambda$ only, up to a dimensional factor Λ^4. The zero-point energy contribution gives the leading contribution to the thermodynamic potential in Eq. (4) and can be evaluated explicitly as, e.g. [33],

$$\begin{aligned}&2N_\mathrm{c}N_\mathrm{f}\int_{p^2\le\Lambda^2}\frac{\mathrm{d}^3p}{(2\pi)^3}\,\omega \\ &= \frac{N_\mathrm{c}N_\mathrm{f}\Lambda^4}{8\pi^2}\left[\sqrt{1+\xi^2}\,(2+\xi^2) + \frac{\xi^4}{2}\ln\left|\frac{\sqrt{1+\xi^2}-1}{\sqrt{1+\xi^2}+1}\right|\right] \\ &\simeq \frac{N_\mathrm{c}N_\mathrm{f}\Lambda^4}{4\pi^2}\big(1+\xi^2\big) + O(\xi^2)\,.\end{aligned} \tag{5}$$

Note that we do not loose the generality of our analysis by assuming small $\xi=M/\Lambda$ because we are only interested in the onset of chiral phase transition where ξ starts taking a finite value from zero. With the expansion in ξ the thermodynamic potential simplifies, to wit,

$$\beta\Omega/V \simeq -\frac{N_\mathrm{c}N_\mathrm{f}\Lambda^4}{4\pi^2}\left[1+\left(1-\frac{2\pi^2}{N_\mathrm{c}N_\mathrm{f}\,\lambda_\Lambda\Lambda^2}\right)\xi^2\right], \tag{6}$$

where we have dropped the higher order terms in ξ. The critical coupling associated with the second-order phase transition should correspond to a point at which the curvature of the thermodynamic potential crosses zero. In order to have a non-zero ξ the potential curvature should be negative and this condition leads to an inequality [33],

$$\lambda_\Lambda\Lambda^2 > \frac{2\pi^2}{N_\mathrm{c}N_\mathrm{f}}\,. \tag{7}$$

This is the condition for the NJL model to accommodate for spontaneous chiral symmetry breaking. Seemingly this depends on the UV cutoff scale Λ. However, as we have already argued above, Λ relates to Λ_QCD in the current effective field theory set-up.

Finite temperature effects are taken into account in a straightforward extension. The full dependence including the finite-μ_q effect will be considered in the numerical analysis in Sec. III. Again we aim at simplicity and analytically estimate the finite-T corrections. This leads to simple understanding of how the chiral phase transition takes place within this effective model. Since we are interested in the regime with infinitesimal ξ, we can make use of the high-T expansion for $T\gg M$, which yields the following thermodynamic potential,

$$\beta\Omega/V \simeq -\frac{N_\mathrm{c}N_\mathrm{f}\Lambda^4}{4\pi^2}\left\{1+\left[1-\frac{2\pi^2}{N_\mathrm{c}N_\mathrm{f}\,\lambda_\Lambda\Lambda^2}-\frac{\pi^2}{3}\left(\frac{\Lambda}{T}\right)^2\right]\xi^2\right\}. \tag{8}$$

Then, in the same way as the condition (7) has been derived, we see that spontaneous chiral symmetry breaking requires,

$$\lambda_\Lambda\Lambda^2 > \frac{2\pi^2}{N_\mathrm{c}N_\mathrm{f}}\left[1-\frac{\pi^2}{3}\left(\frac{\Lambda}{T}\right)^2\xi^2\right]. \tag{9}$$

In the effective model studies, usually, the four-Fermi coupling is fixed by observables in the vacuum. For a given λ_Λ that satisfies the above inequality, we can read the critical temperature directly from Eq. (9) as

$$T_\mathrm{c} = \sqrt{\frac{3\Lambda^2}{\pi^2} - \frac{6}{N_\mathrm{c}N_\mathrm{f}\lambda_\Lambda}}\,. \tag{10}$$

We readily confirm that Eq. (10) gives a conventional value for the critical temperature, i.e. $T_\mathrm{c}=175$ MeV by plugging-in the standard NJL-model parameters, e.g. [33]: $\Lambda=631$ MeV and $\lambda_\Lambda/2=0.214\ \mathrm{fm}^2$.

B. Effects of the magnetic field

We proceed by introducing an external magnetic field $\boldsymbol{B}$. In the present work we restrict ourselves to spatially homogeneous and temporally constant $\boldsymbol{B}$ fields. In the presence of $\boldsymbol{B}$ (along the z-axis) the transverse momenta (i.e. the x and y components) of spin-1/2 particles with electric charge q are quantized into the Landau levels and

the momentum integration with spin sum of a general function $f(\omega)$ is replaced as

$$2\int_{p^2\le\Lambda^2}\frac{\mathrm{d}^3p}{(2\pi)^3}\,f(\omega)\;\longrightarrow\;2\int_{\Lambda,B}\frac{\mathrm{d}^3p}{(2\pi)^3}\,f(\omega_n)$$
$$\equiv\frac{|qB|}{2\pi}\sum_{n=0}^{N_{\Lambda,B}}\alpha_n\int_{p^2\le\Lambda^2}\frac{\mathrm{d}p_z}{2\pi}\,f\big(\sqrt{p_z^2+2|qB|n+M^2}\big)\,, \tag{11}$$

where 2 in the left-hand side is the spin degeneracy, which is replaced by the spin-degeneracy factor α_n that is 1 for $n=0$ (Landau zero-mode) and 2 otherwise. In the second line, $p^2=p_z^2+2|qB|n$ and $N_{\Lambda,B}=\theta_g[\Lambda^2/(2|qB|)]$, where $\theta_g[n+x]=n$ for $n\in\mathbb{Z}$ and $0<x<1$.

Now, let us continue our analytical consideration taking the simplest limit of large magnetic field, more specifically $2|qB|>\Lambda^2$. In this particular limit only the Landau zero-mode contributes as $\theta_g[\Lambda^2/(2|qB|)]=0$ and the lowest Landau level approximation (LLLA) is exact. Note that this should be already a rather quantitative approximation for heavy-ion collisions as the magnetic field strength there is of order of $\Lambda_{\rm QCD}$ which is related to our cutoff scale Λ. In any case we shall also consider general magnetic field within our numerical calculations. In the LLLA, at $\mu_{\rm q}=0$, we can express the thermodynamic potential as

$$\beta\Omega/V=-N_{\rm c}\sum_{f=u,d}\frac{|q_fB|}{2\pi}\int\frac{\mathrm{d}p_z}{2\pi}\Big[\omega_0 + 2T\ln\big(1+\mathrm{e}^{-\beta\omega_0}\big)\Big]+\frac{M^2}{2\lambda_\Lambda}\,. \tag{12}$$

Here we defined $\omega_0=\sqrt{p_z^2+M^2}$ and the quark electric charges are $q_u=(2/3)e$ and $q_d=-(1/3)e$. From this form of the thermodynamic potential one can easily understand the essence of the Magnetic Catalysis. At $T=0$ we can expand the zero-point energy for small $\xi=M/\Lambda$, as we did previously, to find the thermodynamic potential up to $\mathcal{O}(\xi^2)$ as

$$\beta\Omega/V\simeq-N_{\rm c}\sum_{f=u,d}\frac{|q_fB|\Lambda^2}{4\pi^2}\Big[1+\Big(\ln\frac{2}{\xi}+\frac{1}{2}\Big)\xi^2\Big]+\frac{\Lambda^2}{2\lambda_\Lambda}\xi^2\,. \tag{13}$$

As we have already argued, the sign of the curvature determines whether chiral symmetry is spontaneously broken or not. The remarkable feature in the LLLA is that $\ln(1/\xi)$ in the coefficient of ξ^2 is positive and arbitrarily large for $\xi\to0$ and thus it can eventually overcome $\Lambda^2/(2\lambda_\Lambda)$ from the last term. This means that chiral symmetry is always broken however small λ_Λ is. The important point is that such a logarithmic term appeared in the coefficient of ξ^4 in Eq. (5) when $\boldsymbol{B}$ was not applied. In the LLLA with strong $\boldsymbol{B}$ the phase-space volume is suppressed and ξ^4 is reduced to $(|q_fB|/\Lambda^2)\xi^2$. Because $\ln(1/\xi)$ changes its sign from positive to negative for large ξ, the thermodynamic potential (13) has a minimum as a function of ξ that solves the gap equation. In fact, by taking the derivative, we can write down the gap equation, $-N_{\rm c}\sum_f(|q_fB|\Lambda^2/2\pi^2)\ln(2/\xi)+\Lambda^2/\lambda_\Lambda=0$, whose solution ξ_0 or the corresponding constituent mass is

$$M_0=\xi_0\Lambda=2\Lambda\exp\bigg(-\frac{2\pi^2}{N_{\rm c}\,\lambda_\Lambda\sum_f|q_fB|}\bigg)\,. \tag{14}$$

This expression for the condensate is quite analogous to the superconducting gap in the BCS theory. We can see that the critical temperature at which the condensate melts is also given by the same relation as the one known in the BCS theory.

We can carry out the high-T expansion in the same way as previously using

$$\int_{-\infty}^{\infty}\frac{\mathrm{d}p_z}{2\pi}\ln(1+\mathrm{e}^{-\beta\omega_0})\simeq\frac{\pi T}{12}+\frac{\Lambda^2}{4\pi T}\Big(\ln\frac{\Lambda\xi}{\pi T}+\gamma-\frac{1}{2}\Big)\xi^2\,, \tag{15}$$

up to $\mathcal{O}(\xi^2)$. Interestingly enough, a logarithmic term proportional to $\xi^2\ln(1/\xi)$ appears from this finite-T integration as well as the vacuum contribution that we already mentioned. We can make sure that these logarithmic singularities exactly cancel out and the Magnetic Catalysis is lost at finite T. This trend had been reported in the literature [25] and was found also in the context of the Magnetic Catalysis [34]. In the RG analysis in Sec. III the cancellation of the IR singularities will be reconfirmed in a more transparent manner.

The curvature of the thermodynamic potential no longer has a logarithmic singularity at finite T and the critical coupling constant becomes finite again. This is actually the reason why we can expect a chiral phase transition at a certain temperature even in the LLLA calculation with strong $\boldsymbol{B}$. After all, the thermodynamic potential (13) receives the finite-T corrections as

$$\beta\Omega/V\simeq-N_{\rm c}\sum_f\frac{|q_fB|\Lambda^2}{4\pi^2}\bigg\{1+\frac{\pi^2}{3}\Big(\frac{T}{\Lambda}\Big)^2 + \bigg[\ln\Big(\frac{2\mathrm{e}^\gamma\Lambda}{\pi T}\Big)-\frac{2\pi^2}{N_{\rm c}\lambda_\Lambda\sum_f|q_fB|}\bigg]\xi^2\bigg\}\,. \tag{16}$$

The zero of the coefficient of ξ^2 gives a condition for the critical coupling or the critical temperature as obtained in Eq. (10). In this case of the LLLA we arrive at

$$T_{\rm c}=\frac{2\mathrm{e}^\gamma\Lambda}{\pi}\exp\bigg(-\frac{2\pi^2}{N_{\rm c}\,\lambda_\Lambda\sum_f|q_fB|}\bigg)=\frac{\mathrm{e}^\gamma}{\pi}M_0\,. \tag{17}$$

This relation between the condensate at $T=0$ and the melting temperature is perfectly identical to the results from the BCS theory. If the coupling constant λ_Λ is infinitely large, all expressions appear very simple; the critical temperature without $\boldsymbol{B}$ is read from Eq. (10) as $T_{\rm c}=(\sqrt{3}/\pi)\Lambda\simeq0.551\Lambda$, and that at strong $\boldsymbol{B}$ is from Eq. (17) as $T_{\rm c}=(2\mathrm{e}^\gamma/\pi)\Lambda\simeq1.13\Lambda$. Therefore the critical temperature is indeed raised by the $\boldsymbol{B}$ effect, which is in qualitative agreement with effective model calculations.

III. RENORMALIZATION GROUP ANALYSIS

In the previous section we have discussed the standard mean-field analysis where quark quantum fluctuations are taken into account at one loop. In the present section we extend the analysis beyond the one-loop level by means of RG-techniques. This also allows us to formulate the physics mechanism of the chiral phase transition from a different and rather simple point of view. To that end we here introduce an IR-cutoff term into the Lagrangian and derive a functional RG equation for the free energy or effective action, the Wetterich equation [35]. In this approach the kinetic term is modified in momentum space in order to suppress momentum modes below the given infrared (IR) cutoff scale k. This leads to an infrared regularized free energy or effective action $\Gamma_k[\psi,\bar{\psi}]$ which reduces to the thermodynamic potential Ω at vanishing IR cutoff $k=0$ on the equations of motion (EoM) of $\psi,\bar{\psi}$, that is $\Omega=\Gamma_{k=0}|_{\rm EoM}$. For the sake of simplicity we resort to a three-dimensional IR-cutoff which allows us to perform the Matsubara summation analytically. Then the fermion propagator in Euclidean space takes the following form,

$$G(p)=\frac{1}{\gamma_4 p_4+\vec{\gamma}\cdot\vec{p}\,[1+r_k(\vec{p})]}\,. \tag{18}$$

Here $r_k(\vec{p})$ is the cutoff function with $r_k(\vec{p})\sim k/|\vec{p}|$ for $\vec{p}^2<k^2$ and $r_k(\vec{p})\to 0$ for $\vec{p}^2>k^2$. Note also that the dimensionless shape of r_k is genuinely a function of $|\vec{p}|/k$. Since we are interested in the chiral properties of QCD, we have avoided implementing the cutoff function as a momentum-dependent mass term but in the kinetic term. The former cutoff explicitly breaks chiral symmetry and would have similar effects on chiral properties as the Wilson mass term has on the lattice. The scale-dependence of Γ_k is then encoded in the flow equation, schematically written as

$$\partial_t\Gamma_k[\psi,\bar{\psi}]=-{\rm Tr}\left(\frac{1}{\Gamma_k^{(1,1)}[\psi,\bar{\psi}]+\vec{\gamma}\cdot\vec{p}\,r_k}\,\vec{\gamma}\cdot\vec{p}\,\partial_t r_k\right),$$
$$\Gamma_k^{(1,1)}[\psi,\bar{\psi}]=\frac{\overrightarrow{\delta}}{\delta\bar{\psi}}\Gamma_k[\psi,\bar{\psi}]\frac{\overleftarrow{\delta}}{\delta\psi}\,, \tag{19}$$

where $t=\ln(k/\Lambda)$ is the logarithmic IR scale with reference scale Λ and the trace Tr sums over momenta, Dirac indices, flavors. (For QCD-related reviews, see Refs. [30, 36–39]). In the present work we ignore the effects of the multi-scattering of quarks, which is phase-space suppressed. We rush to add that this argument gets weaker at higher densities. For the time being we make the additional approximation of a local effective four-Fermi vertex λ_k, which will be relaxed in the next section. This leads us to the following simple Ansatz for the effective action,

$$\Gamma_k=\int{\rm d}^4x\left(\bar{\psi}{\rm i}\partial\!\!\!/\psi+\frac{1}{2}\bar{\psi}_i^{a\alpha}\psi_j^{b\alpha}{\Gamma_k}_{ijlm}^{abcd}\bar{\psi}_l^{c\beta}\psi_m^{d\beta}\right), \tag{20}$$

where ${\Gamma_k}_{ijlm}^{abcd}$ is given by Eq. (2) with $\Lambda\to k$. This form is substituted into the flow equation (19) and we take the functional derivatives. The left-hand side of the flow equation is then,

$$\begin{aligned}\partial_t\Gamma_k^{(2,2)}&\equiv\partial_t\frac{\overrightarrow{\delta}}{\delta\bar{\psi}_i^{a\alpha}(x)}\frac{\overrightarrow{\delta}}{\delta\bar{\psi}_l^{c\gamma}(z)}\Gamma_k\frac{\overleftarrow{\delta}}{\delta\psi_j^{b\beta}(y)}\frac{\overleftarrow{\delta}}{\delta\psi_m^{d\delta}(w)}\\&=\delta(x-y)\,\delta(y-z)\,\delta(z-w)\\&\quad\times\left(\delta^{\alpha\beta}\delta^{\gamma\delta}\partial_t{\Gamma_k}_{ijlm}^{abcd}-\delta^{\alpha\delta}\delta^{\beta\gamma}\partial_t{\Gamma_k}_{imlj}^{adcb}\right).\end{aligned} \tag{21}$$

The right-hand side is a bit complicated. There arise twelve terms, six of which are proportional to $\delta^{\alpha\beta}\delta^{\gamma\delta}$ and other six proportional to $\delta^{\alpha\delta}\delta^{\beta\gamma}$, respectively. Here, let us focus on the part of $\delta^{\alpha\beta}\delta^{\gamma\delta}$ only. In addition, because we aim to have the flow equation for λ_k, we can simplify the calculation by contracting the Dirac and the flavor indices of external legs, namely, $\delta_{ij}\delta_{lm}\delta^{ab}\delta^{cd}{\Gamma_k}_{ijlm}^{abcd}=16N_{\rm f}^2\,\lambda_k$. Then six terms are no longer independent but only three remain distinguishable. The flow equation is eventually given by

$$\begin{aligned}\partial_t{\Gamma_k}_{iill}^{aacc}&=2N_{\rm c}{\rm Tr}\left[G_{jm}\Gamma_{mpii}^{bdaa}G_{pq}\Gamma_{qrll}^{dbcc}G_{rs}(\vec{\gamma}\cdot\vec{p})_{sj}\;\partial_t r_k\right]\\&\quad-2{\rm Tr}\left[G_{jm}\Gamma_{miip}^{baad}G_{pq}\Gamma_{qrll}^{dbcc}G_{rs}(\vec{\gamma}\cdot\vec{p})_{sj}\;\partial_t r_k\right]\\&\quad-2{\rm Tr}\left[G_{jm}\Gamma_{mpii}^{bdaa}G_{pq}\Gamma_{qllr}^{dccb}G_{rs}(\vec{\gamma}\cdot\vec{p})_{sj}\;\partial_t r_k\right],\end{aligned} \tag{22}$$

when no momentum is carried by any external legs. In Eq. (22) we have also dropped the subscript k on the vertices. There are four different types of Feynman diagrams that contribute to the flow equation as displayed in Fig. 1. Here (a) corresponds to the first term in the right-hand side of Eq. (22), (b) and (c) to the second term, and (d) to the third term.

After some calculations we can arrive at the following form of the flow equation with $N_{\rm f}=2$;

$$\begin{aligned}\partial_t\lambda_k=-4\,\left(2N_{\rm c}+\frac{3}{4}\right)\lambda_k^2\sum_{f=u,d}\sum\!\!\!\!\!\!\int_{T,B}\frac{{\rm d}^4p}{(2\pi)^4}\,|\vec{p}|\partial_t r_k(\vec{p})\\\times\frac{|\vec{p}|\,[1+r_k(\vec{p})]}{\left\{p_4^2+\vec{p}^2[1+r_k(\vec{p})]^2\right\}^2}\,,\end{aligned} \tag{23}$$

where the factor four in Eq. (23) originates in the trace of the Dirac index and the factor $2N_{\rm c}$ comes from (a) which is the leading diagram in the $1/N_{\rm c}$ expansion. The factor $3/4=1-1/4$ is a combination of 1 from the diagrams (b) and (c) and $1/4$ from the diagram (d).

Before we come to the explicit computations we would like to discuss the structure of the flow in Eq. (23) as it already reveals a lot of interesting properties of the flow and is also important for the computations and the interpretation of the results. The flow (23) has a total t-derivative structure and hence leads to results at $k=0$ that are independent of the chosen regulator r_k up to (re-)normalizations at the initial scale Λ. To see this more clearly we rewrite it as a flow for $1/\lambda_k$, to wit,

$$\partial_t\frac{1}{\lambda_k}=-\partial_t\left[\Pi_k(0)-\Pi_\Lambda(0)\right], \tag{24}$$

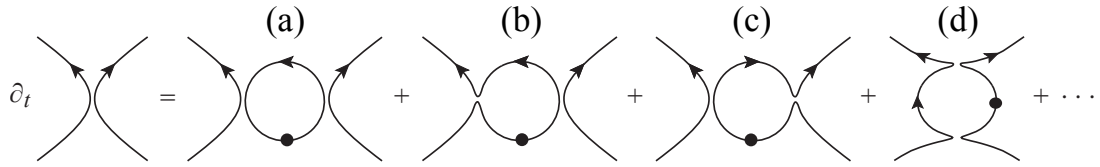

FIG. 1. Diagrammatic representation of the flow equation for the four-Fermi interaction. At each vertex the color index is contracted along the connected lines. The ellipses are neglected contributions from higher loop diagrams beyond the Ansatz (20)

.

with

$$\Pi_k(0) \simeq -\sum\!\!\!\!\!\!\int_{T,B} \frac{\mathrm{d}^4p}{(2\pi)^4} \sum_{f=u,d} \frac{2\big(2N_\mathrm{c}+\frac{3}{4}\big)}{p_4^2+\vec{p}^{\,2}\,[1+r_k(\vec{p})]^2}\,. \tag{25}$$

In Eq. (24) we have introduced the subtraction term for having explicitly finite expressions before t-derivatives are taken. In its form (24) the flow is easily integrated and leads to

$$\frac{1}{\lambda_k} = \frac{1}{\lambda_\Lambda} - \big[\Pi_k(0) - \Pi_\Lambda(0)\big]\,. \tag{26}$$

We immediately deduce that the dependence on the regulator drops out at $k = 0$ for consistent choice of λ_Λ; evidently there is no dependence on $r_0(p) \equiv 0$. In turn, $1/\lambda_\Lambda + \Pi_\Lambda(0)$ is required to be Λ-independent, otherwise λ_0 would depend on Λ. The latter condition encodes RG-invariance of the theory, not to be mixed-up with renormalizability. We also deduce from Eq. (26) that in the leading order $1/\lambda_\Lambda \propto -\Pi_\Lambda(0) = c(r_\Lambda)\Lambda^2$. The prefactor depends on the chosen regulator and hence defines the regularization scheme. This is seen more clearly if comparing the dimensionless coupling,

$$\hat{\lambda}_k = \lambda_k k^2\,, \tag{27}$$

at the initial scale Λ for two different regulator $r_k^{(1)}, r_k^{(2)}$. This leads to $\hat{\lambda}_\Lambda^{(1)}/\hat{\lambda}_\Lambda^{(2)} = c^{(2)}/c^{(1)}$. For agreeing physics scales the above ratio should be one and we identify $\Lambda^{(2)} = c^{(1)}/c^{(2)}\Lambda$ with $\Lambda^{(1)} = \Lambda$. In other words, we expect that the equivalence of the mean-field inequality (7) depends on the chosen regulator simply by a multiplicative factor in front of $\hat{\lambda}$;

$$\lambda_\Lambda \Lambda^2 > \frac{c(r_\Lambda)}{c(r_\Lambda^{\mathrm{sharp}})}\frac{2\pi^2}{N_\mathrm{c}N_\mathrm{f}}\,. \tag{28}$$

where $c(r_\Lambda^{\mathrm{sharp}})$ stands for the implicit regulator used in the mean-field computation, that is the three-dimensional sharp cutoff; $r_k^{\mathrm{sharp}}(p^2) = \theta(p^2 - k^2)$. We emphasize once more that this only reflects the dependence of λ_Λ on the chosen RG-scheme.

In summary we conclude that λ_0 does not depend on r_Λ either and any regulator-dependence is removed. We emphasize that this is a particularity of the present approximation and hinges on its explicit total derivative structure. Such approximations are singled-out as regulator-independent and also related to optimization criteria that amongst other properties (re-)enforce total derivative structures for the flows; for more detailed discussions, see Ref. [38, 40]. For later purpose we also resolve Eq. (26) for λ_k,

$$\lambda_k = \frac{\lambda_\Lambda}{1 - \lambda_\Lambda[\Pi_k(0) - \Pi_\Lambda(0)]}\,. \tag{29}$$

Equation (26) elucidates the resummation structure of the flow. It encodes a bubble resummation of the diagrams in Fig. 1. This is seen within a diagrammatic expansion of Eq. (26) in orders of λ_Λ,

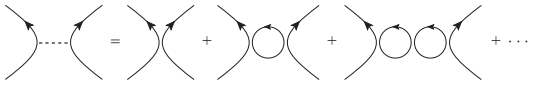

(30)

If we interpret the dashed line on the left-hand side as a meson propagator it results simply from the bubble resummation shown in Fig. 30. The first term on the right-hand side, i.e. the tree-level diagram, gives λ_Λ and hence a tree-level meson propagator λ_Λ. The second term comes from the one-loop polarization, that is, $\lambda_\Lambda^2\Pi_k(0)$, where the momentum argument is zero because we only consider the situation that all external legs bring no momentum insertion. If we lower the temperature towards the hadronic phase the four-Fermi vertex function has to diverge at the phase transition as it contains a massless sigma and pion propagation. Indeed, when introducing effective mesonic degrees of freedom with the σ and $\vec{\pi}$ coupling to the related quark bilinears, it can be shown that the meson mass is proportional to $1/\lambda_k$. This makes it clear that a single pole in the four-Fermi coupling does not merely signal the validity bound of the approximation but rather the onset of condensation.

This ends our discussion of the formal properties of the flow (23) and we proceed on how to practically solve it. As we have argued, its solution does not depend on the chosen regulator. This fully justifies the choice taken already in restricting ourselves to three-dimensional regulators. It allows us to perform the p_4 integration or summation with respect to the Matsubara frequency most easily. The result is

$$T\sum_n \frac{\omega}{(p_4^2+\omega^2)^2} = \frac{1}{4\omega^2} + \frac{\mathrm{d}}{\mathrm{d}\omega}\frac{1}{2\omega}\frac{1}{\mathrm{e}^{\beta\omega}+1}\,, \tag{31}$$

with $\omega \equiv |\vec{p}\,|\,|1 + r_k(\vec{p})|$. We still have to specify the three-dimensional regulator, $r_k(p)$, to proceed further. We again utilize the regulator-independence and adopt the three-dimensional flat cutoff, [41], for the sake of simplicity,

$$r_k^{\rm flat}(\vec{p}) = \left(\frac{k}{|\vec{p}|} - 1\right)\theta(k/|\vec{p}| - 1)\,. \tag{32}$$

Such flat cutoffs were first introduced in Ref. [42] for the purpose of optimization are also most useful for analytical studies. It is called "flat" because it renders the spatial dispersion momentum-independent for momenta below the cutoff scale,

$$\omega(r_k^{\rm flat})\theta(k/|\vec{p}| - 1) = k\,, \tag{33}$$

where ω denotes a quantity defined just blow Eq. (31). For momenta $|\vec{p}| < k$, hence, the Matsubara sum in Eq. (31) turns into

$$\frac{1}{2k^2}\left[\frac{1}{2} - \frac{1}{{\rm e}^{\beta k}+1} - \beta k\frac{{\rm e}^{\beta k}}{({\rm e}^{\beta k}+1)^2}\right]. \tag{34}$$

which is completely momentum-independent. The integrand in the four-Fermi flow (23) is also proportional to the scale derivative of the regulator, $\partial_t\, r_k^{\rm flat}(p) = (k/|\vec{p}|)\,\theta(k/|\vec{p}| - 1)$ which limits the integration to momenta $|\vec{p}| < k$ where the integration is trivial. This leads us, particularly when $\boldsymbol{B} = 0$, to

$$\partial_t \Pi_k(0) = \frac{\left(2N_{\rm c} + \frac{3}{4}\right)N_{\rm f}}{3\pi^2}\left[\frac{1}{2} - \frac{1}{{\rm e}^{\beta k}+1} - \beta k\frac{{\rm e}^{\beta k}}{({\rm e}^{\beta k}+1)^2}\right], \tag{35}$$

to be inserted in Eq. (24). In later discussions it also turns out that the choice (33) for $r_k(\vec{p})$ avoids unphysical oscillatory behavior in the flow from the discrete Landau levels. For going beyond the present approximation which we shall do in the last section it is worth noticing that this cutoff is optimized in the high temperature limit, [38, 42], and keeps some of this property also at momentum-independent approximations. For fully momentum-dependent approximations as well as finite magnetic field it introduces momentum non-localities (momentum flows in diagrams) which affect the quantitative accuracy (see Ref. [43]). In short, within the approximations used in the present work the regulator works sufficiently well and has the advantage of analytical tractability. Within extensions of this work we shall aim at quantitative precision and will resort to regulators which maintain momentum locality and minimize the momentum flow.

A. Flow and chiral symmetry breaking

We first concentrate on the relation between the flow of the four-Fermi coupling and chiral symmetry breaking at $T = 0$ and $\boldsymbol{B} = 0$. This gives access to the simple structure and understanding of chiral symmetry breaking within the flow equation approach, and hence serves as a useful example for understanding the results in the presence of medium effects. In order to facilitate the direct comparison with the mean-field results, we shall first discuss the large-$N_{\rm c}$ limit at leading order. Then, only the diagram (a) in Fig. 1 contributes. Note that due to the simple full N_c-dependence of the flow (see Eq. (23)), the limit is easily undone by replacing $N_{\rm c} \to N_{\rm c} + \frac{3}{8}$ in the large $N_{\rm c}$ result. For the flat regulator and $T = 0$ the flow of the vacuum polarization, Eq. (35), is $N_{\rm c}/(3\pi^2)$ and we arrive at

$$\partial_t \lambda_k = -\frac{N_{\rm c}N_{\rm f}\,\lambda_k^2 k^2}{3\pi^2}\,, \tag{36}$$

as well as

$$\lambda_k = \frac{\lambda_\Lambda}{1 + \frac{N_{\rm c}N_{\rm f}\,\lambda_\Lambda}{6\pi^2}(k^2 - \Lambda^2)}\,, \tag{37}$$

with a positive initial coupling λ_Λ. From Eqs. (36) and (37) we infer that lowering k increases λ_k. At $N_{\rm c}N_{\rm f}\,\lambda_\Lambda\Lambda^2/(6\pi^2) = 1$ the coupling diverges and has a single pole. We have already argued that Eq. (28) has to be understood as the onset of spontaneous chiral symmetry breaking, and the occurance of massless mesonic modes. Hence, with the present regulator the condition for spontaneous chiral symmetry breaking, Eq. (28), is given by

$$\lambda_\Lambda\Lambda^2 > \frac{6\pi^2}{N_{\rm c}N_{\rm f}}\,. \tag{38}$$

This result is the counterpart of the condition (7) in the mean-field theory. The discrepancy by a factor 3 relates to the different regularization scheme between the sharp cutoff in the mean-field treatment and the optimized cutoff in the RG analysis. We can identify, roughly speaking, the RG-scale Λ^2 in the present RG study with $3\Lambda^2$ in the mean-field approximation.

The same conclusion can be drawn from a fixed-point argument, directly utilizing Eq. (36); by changing to the dimensionless coupling $\hat{\lambda}$ in Eq. (27) the flow (36) changes to

$$\beta_{\hat{\lambda}} \equiv \partial_t\hat{\lambda}_k = 2\hat{\lambda}_k - \frac{N_{\rm c}N_{\rm f}}{3\pi^2}\,\hat{\lambda}_k^2\,. \tag{39}$$

The β-function in Eq. (39) vanishes at $\hat{\lambda}_* = 6\pi^2/(N_{\rm c}N_{\rm f})$ which is an attractive UV fixed point. Of course, this defines exactly the critical coupling constant given in Eq. (38). If $\hat{\lambda}_\Lambda$ starts from a value above $\hat{\lambda}_*$, the flow grows larger for smaller k, which indicates the spontaneous breaking of chiral symmetry.

With this simple picture of chiral symmetry breaking we proceed to finite temperature T and quark chemical potential $\mu_{\rm q}$. More specifically we search for the critical temperature (or chemical potential) above which chiral

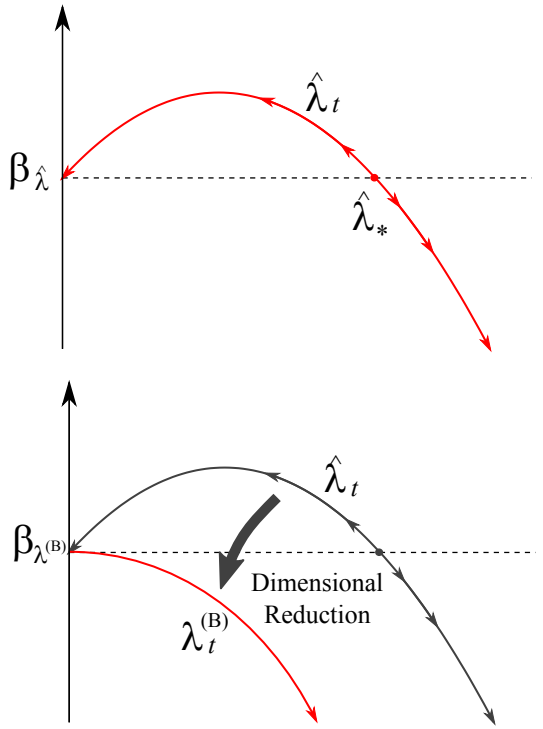

FIG. 2. Flow pattern of the four-Fermi coupling constant without $\boldsymbol{B}$ (upper figure) and with $\boldsymbol{B}$ (lower figure). In the latter case chiral symmetry is always broken as a result of dimensional reduction.

symmetry is restored for a given λ_Λ. The flow equation now receives medium corrections, to wit,

$$\partial_t\hat\lambda_k = 2\hat\lambda_k - \frac{N_{\rm c}N_{\rm f}\,\hat\lambda_k^2}{3\pi^2} \times\left\{1-(1-\partial_t)\big[n(k-\mu_{\rm q})+n(k+\mu_{\rm q})\big]\right\}, \tag{40}$$

where $n(k)=1/(\mathrm{e}^{\beta k}+1)$ is the Fermi-Dirac distribution function. Assume now that the initial coupling exceeds the fixed point coupling at vanishing temperature, i.e., $\hat\lambda_\Lambda > \hat\lambda_*$ with $\hat\lambda_*$ in Eq. (38) and hence $\beta_{\hat\lambda}|_{k=\Lambda} < 0$. we again make contact to the mean-field analysis within a solution of the differential equation (40) at $\mu_{\rm q}=0$. We can readily integrate it to write down the running coupling constant,

$$\lambda_k = \frac{\lambda_\Lambda}{1+\dfrac{N_{\rm c}N_{\rm f}\lambda_\Lambda}{3\pi^2}\displaystyle\int_\Lambda^k {\rm d}k'\,k'\left(1-\frac{2}{\mathrm{e}^{\beta k'}+1}-\frac{2\beta k'\mathrm{e}^{\beta k'}}{(\mathrm{e}^{\beta k'}+1)^2}\right)}\,. \tag{41}$$

Here, because we are interested in $T_{\rm c}$ inferred from the Landau pole associated with the flow of $k\to 0$, we make an approximation of $k\sim 0$ and $\Lambda\sim\infty$ in the matter part and evaluate the integration as

$$\int_\infty^0 {\rm d}k'\,k'\left(-\frac{2}{\mathrm{e}^{\beta k'}+1}-\frac{2\beta k'\mathrm{e}^{\beta k'}}{(\mathrm{e}^{\beta k'}+1)^2}\right)=\frac{\pi^2T^2}{2}\,. \tag{42}$$

Then, the running coupling (41) can be well approximated as

$$\lambda_k = \frac{\lambda_\Lambda}{1+\dfrac{N_{\rm c}N_{\rm f}\,\lambda_\Lambda}{6\pi^2}\big(k^2-\Lambda^2+\pi^2T^2\big)}\,, \tag{43}$$

from which the Landau pole position leads to the condition for the critical temperature;

$$T_{\rm c}=\sqrt{\frac{\Lambda^2}{\pi^2}-\frac{6}{N_{\rm c}N_{\rm f}\,\lambda_\Lambda}}\,. \tag{44}$$

With the cutoff replaced as $\Lambda^2\to 3\Lambda^2$, this is precisely consistent with the mean-field result in Eq. (10).

B. Magnetic Catalysis

We introduce finite $\boldsymbol{B}$ using Eq. (11) and inserting appropriate spin projection operators in the trace of the Dirac indices. In the LLLA we can easily understand the Magnetic Catalysis from the flow pattern. At $T=0$ the flow equation in the strong $\boldsymbol{B}$ limit takes the following form;

$$\partial_t\lambda_k = -\frac{N_{\rm c}}{2\pi^2}\sum_f |q_fB|\,\lambda_k^2 \tag{45}$$

with $t=\ln(k/\Lambda)$, which we can solve immediately as

$$\lambda_k=\frac{\lambda_\Lambda}{1+\dfrac{N_{\rm c}\,\lambda_\Lambda}{2\pi^2}\displaystyle\sum_f|q_fB|\,t}\,. \tag{46}$$

Because $t=\ln(k/\Lambda)$ ranges from 0 ($k=\Lambda$) to $-\infty$ ($k=0$), the denominator of Eq. (46) inevitably hits the Landau pole in the flow of k in sharp contrast to the zero-$\boldsymbol{B}$ case. The existence of the Landau pole implies that the chiral symmetric state is always unstable and so chiral symmetry should be broken in the LLLA. This is nothing but the manifestation of the Magnetic Catalysis.

In the same way as previously, we can understand this from the behavior of the β-function of λ_k. In contrast to Eq. (39) the mass dimension of λ_k is now balanced by not k^2 but $|q_fB|$ because of the dimensional reduction. Therefore, the first term in Eq. (39), $2\hat\lambda_k$, does not appear, and the behavior of the β-function changes as sketched in Fig. 2. More specifically, introducing a dimensionless coupling by $\lambda_k^{(\rm B)}\equiv(\sum_f|q_fB|/2\pi^2)\lambda_k$, the flow equation reads,

$$\beta_{\lambda^{(\rm B)}}\equiv -N_{\rm c}\big(\lambda_t^{(\rm B)}\big)^2\,. \tag{47}$$

It is obvious from this that the flow goes to infinity regardless of the initial point of λ_Λ. From the solution (46) we can easily locate the Landau pole at

$\ln(k_0/\Lambda) = -2\pi^2/(N_c\lambda_\Lambda \sum_f |q_f B|)$, that characterizes the typical scale for the condensate, i.e.

$$M_0 \propto k_0 = \Lambda \exp\left(-\frac{2\pi^2}{N_c\lambda_\Lambda \sum_f |q_f B|}\right), \qquad (48)$$

which gives an estimate for the chiral condensate up to an overall coefficient. We note that the exponential factor is identical with that in Eq. (14) since it does not depend on Λ which carries the scheme-dependence. It does depend on $\sum_f |q_f B|\lambda_\Lambda$ which is already dimensionless.

C. Finite temperature and density

It is an interesting question how the chiral phase transition at finite T and/or μ_q is possible even in the LLLA in the RG formulation. In other words, the question is how the Magnetic Catalysis is lost and chiral restoration becomes possible when a finite T and/or μ_q is turned on. The running coupling constant has extra contributions at finite T as

$$\lambda_k = \lambda_\Lambda\left[1 - \frac{N_c\lambda_\Lambda}{2\pi^2}\sum_f |q_f B| \int_k^\Lambda \frac{dk'}{k'} \times \left(1 - \frac{2}{e^{\beta k'}+1} - \frac{2\beta k' e^{\beta k'}}{(e^{\beta k'}+1)^2}\right)\right]^{-1}. \qquad (49)$$

As we did before, we can approximate $k \simeq 0$ in the integration range as long as we are interested in T_c only, and also take $\Lambda \simeq \infty$, which makes the last term in the integration part in Eq. (49) as

$$\int_0^\infty \frac{dk'}{k'} \frac{2\beta k' e^{\beta k'}}{(e^{\beta k'}+1)^2} = 1\,. \qquad (50)$$

The first and the second terms are more interesting than the third one. The Magnetic Catalysis stems from the IR singularity from $\int_k^\Lambda dk'/k' = -\ln(k/\Lambda)$, while the finite-$T$ contribution exactly cancels the IR singularity as explicitly checked as

$$\int_0^\Lambda \frac{dk'}{k'}\left(1 - \frac{2}{e^{\beta k'}+1}\right) = \int_0^{\beta\Lambda} \frac{dx}{x}\frac{e^x - 1}{e^x + 1} \simeq \ln(1.13\beta\Lambda). \qquad (51)$$

This recovers the same expression for T_c as Eq. (17) up to the prefactor that again depends on the regularization scheme; from the zero of the denominator in Eq. (49) we can infer in the LLLA,

$$T_c = 0.42\Lambda \exp\left(-\frac{2\pi^2}{N_c\lambda_\Lambda \sum_f |q_f B|}\right). \qquad (52)$$

We can relax the LLLA and solve λ_k for arbitrary $\boldsymbol{B}$ at finite T and μ_q numerically. We can write the running coupling constant down as follows;

$$\lambda_k = \lambda_\Lambda\left[1 - \frac{N_c\lambda_\Lambda}{2\pi^2}\sum_f |q_f B| \int_k^\Lambda \frac{dk'}{k'} \times \sum_{n=0}^{N_{k,B}} \alpha_n \sqrt{1 - \frac{2|q_f B|n}{k'^2}}\Big\{1 - n(k'-\mu_q) - n(k'+\mu_q) + k\partial_k\big[n(k'-\mu_q) + n(k'+\mu_q)\big]\Big\}\right]^{-1}. \qquad (53)$$

In this expression n can take a positive integer up to $N_{k,B} = \theta_g[k^2/(2|q_f B|)]$. From the zero of the denominator, the critical coupling constant λ_* is fixed as a function of T, μ_q, and B in unit of Λ, that is,

$$\frac{1}{\lambda_*} = \frac{N_c}{2\pi^2}\sum_f |q_f B| \int_0^1 \frac{dx}{x} \sum_{n=0}^{N_{x\Lambda,B}} \alpha_n \sqrt{1 - \frac{2|q_f B|n}{x^2\Lambda^2}} \times \left(1 - \frac{1}{e^{\beta(x\Lambda-\mu_q)}+1} - \frac{1}{e^{\beta(x\Lambda+\mu_q)}+1} - \frac{\beta x\Lambda\, e^{\beta(x\Lambda-\mu_q)}}{(e^{\beta(x\Lambda-\mu_q)}+1)^2} - \frac{\beta x\Lambda\, e^{\beta(x\Lambda+\mu_q)}}{(e^{\beta(x\Lambda+\mu_q)}+1)^2}\right). \qquad (54)$$

The numerical results are shown in Fig. 3 at zero density (upper) and at finite density (lower). We here like to point out that the numerical results are entirely smooth. This nice feature is attributed to the choice of the optimized cutoff function. In fact, the Landau level summation stops at $n = N_{k,B}$ but the contribution in the vicinity of this upper bound is vanishingly small due to the weight $\sqrt{1 - 2|q_f B|n/k'^2}$. In other words, the optimized form (32) is a small regularization function, though it involves Heaviside's step function.

In the upper panel of Fig. 3 we can confirm the Magnetic Catalysis from the behavior of decreasing λ_* toward zero with increasing $|eB|$ at $T = 0$. In view of the upper panel of Fig. 3, however, the Magnetic Catalysis, $\lambda_* = 0$, is slowly reached for asymptotically large $\boldsymbol{B}$ only. We already mentioned that the LLLA is exact for $2|qB| > \Lambda^2$. In fact, the curve at $T \simeq 0$ in Fig. 3 is not the result at strict zero-T but at $T = 10^{-5}\Lambda$ for numerical stability. As soon as finite T is introduced, λ_* is significantly pushed up and the Magnetic Catalysis can occur only in the limit of $\boldsymbol{B} \to \infty$, though $\lambda_* = 0$ for any $\boldsymbol{B}$ at strict zero-T.

It is also evident from the lower panel of Fig. 3 that the Magnetic Catalysis is lost immediately at finite μ_q and λ_* never approaches zero even at $T = 0$ then. More interestingly, we can see in the figure that λ_* increases, meaning that chiral symmetry breaking weakens, with increasing $\boldsymbol{B}$ contrary to the trend at $\mu_q = 0$. These are quite suggestive results implying that the modification in the QCD phase boundaries induced by $\boldsymbol{B}$ weakens at higher temperature, and $\boldsymbol{B}$ would rather favor chiral restoration for cold and dense quark matter.

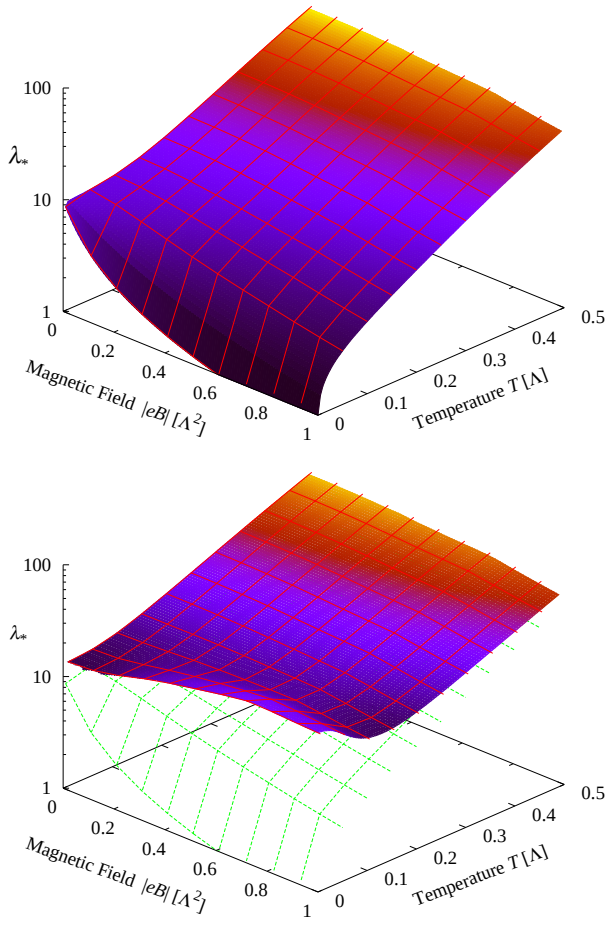

FIG. 3. Critical coupling constant λ_* of chiral symmetry breaking and restoration as a function of the temperature T and the magnetic field $|eB|$ in unit of Λ for zero quark chemical potential $\mu_q = 0$ (upper) and $\mu_q = 0.3\Lambda$ (lower; with zero-density results shown for reference).

IV. NON-LOCAL VERTEX AND RESUMMATION

So far, we have worked in the leading order of the $1/N_c$-expansion which amounts to neglecting the diagrams (b),(c),(d) in Fig. 1. Once they are included in the calculation, the overall coefficient is modified from $2N_c$ to $2N_c + \frac{3}{4}$, leaving aside the complexity due to isospin symmetry breaking by $\boldsymbol{B}$.

Hence, in practice, the sub-leading contributions have the minor effect of changing the overall factor. Strictly speaking, however, this is not the end of the story. The running coupling constant has an interpretation in terms of the meson propagation in the intermediate state as illustrated in the schematic representation (30). Because we defined λ_k from the four-point vertex function with zero momentum insertion from external legs, we could describe the meson propagation only for zero momentum, as explicitly indicated in Eq. (24). Such a treatment is correct for (a), but not adequate for (b), (c), and (d). In this section we will discuss qualitative effects of the momentum-dependent (i.e. non-local) vertices mediated by the meson propagation.

A. Partial resummation

Using the graphical representation (30) we can express the diagram (d) as a box-type diagram as follows;

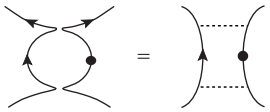

(55)

Here, it is clear that two meson propagators must carry the internal loop momentum and λ_k in the diagram should be replaced by the momentum-dependent coupling $\lambda_k(p)$. For the diagrams (b) and (c) as well as (a) we can utilize a similar representation with non-local vertices.

One might have thought of a different type of the box diagram, that is, the one with the s- and t-channels flipped. However, such a diagram does not give an additional contribution because, as we have explained below Eq. (21), the color structure is decomposed into two pieces. We are now handling the part of $\delta^{\alpha\beta}\delta^{\gamma\delta}$ and the flipped diagram belongs to another part of $\delta^{\alpha\delta}\delta^{\beta\gamma}$. This is a crucial difference from the box diagram in terms of flavor indices encountered, for example, in the QED analysis [44].

To take account of these effects properly, therefore, we should use the momentum-dependent coupling constant and it is natural to anticipate the following replacement;

$$\lambda_k = \frac{\lambda_\Lambda}{1-\lambda_\Lambda[\Pi_k(0)-\Pi_\Lambda(0)]} \quad \Rightarrow \quad \lambda_k(p) = \frac{\lambda_\Lambda}{1-\lambda_\Lambda[\Pi_k(p)-\Pi_\Lambda(p)]}\,. \tag{56}$$

This is nothing but the coupling arising from a full momentum-dependent bubble resummation and can be achieved within 2PI-approximations to the flow [40].

Within such a momentum-dependent approximation we should discuss anew the validity of the LLLA. We can imagine the complexity from a simple fact that the energy dispersion of charged quarks is Landau quantized, while neutral mesons consisting of those quarks do not feel $\boldsymbol{B}$ at all and thus no Landau quantization occurs if they are tightly bound. We can indeed understand this from Eq. (56); the point is that $\Pi_k(p)$ in Eq. (56) is the polarization in the presence of the IR cutoff k, that is, the IR modes with $p^2 + 2|q_f B|n < k^2$ are massive and do not run in the loop, which makes $\Pi_k(p)$ dependent on k. As long as $|q_f B|$ is well smaller than Λ^2, the magnetic field cannot resolve the internal structure of bound-state system and the LLLA is not sufficient. In this case the apparent suppression of quark propagator

by $|q_f B|$ is canceled by the energy denominator in the polarization calculation. On the other hand, if $|q_f B|$ is greater than Λ^2, all non-zero Landau modes ($n \neq 0$) are outside of the IR cutoff region and only the zero-mode can depend on k. Therefore, only the zero-mode survives in $\Pi_k(p) - \Pi_\Lambda(p)$. Roughly speaking, the transverse motion of neutral mesons gets frozen if the magnetic field strength is larger than the inverse squared of the meson size and this could be regarded as B-induced dissociation or deconfinement. Such a transitional change of meson structure as a function of B is a very interesting theoretical question beyond the scope of this present work.

Let us just assume that $|q_f B|$ is sufficiently large and the LLLA holds in the computation of $\Pi_k(p) - \Pi_\Lambda(p)$. Then, after some calculations, we find,

$$\Pi_k(p) - \Pi_\Lambda(p) \simeq -\frac{N_{\rm c}}{2\pi^2}\sum_f |q_f B|\left[\ln(k/\Lambda) + \frac{|p_z|}{2k} + \frac{3p_4^2}{8k^2} + \frac{p_z^2}{8k^2}\right], \quad (57)$$

where we expanded the results in terms of p_4/k and p_z/k and took $\Lambda \gg p_4, p_z$ to neglect p_4/Λ and p_z/Λ. We can immediately confirm that we can recover the running coupling (46) by plugging Eq. (57) into Eq. (56) at zero momenta. Because p_z is the loop momentum in the diagrams (b)–(d) which is cutoff at k by the quark propagator, p_z and p_4 are certainly smaller than k. Since the introduction of k explicitly breaks Lorentz symmetry, Eq. (57) is a function of not only $p_4^2 + p_z^2$ but also $|p_z|$ independently. We have introduced $r_k(\vec{p})$ in the quark propagator to suppress the IR modes with $|\vec{p}| < k$ and, somehow, the meson propagator should have the IR cutoff generated dynamically. Then, the spatial momentum of meson is shifted up by the IR cutoff k. To take account of this cutoff effect qualitatively, it would suffice to keep the linear term only in Eq. (57). The running coupling with momentum dependence is then expressed as

$$\lambda_k(p) = \frac{\lambda_k}{1 + \dfrac{N_{\rm c}\lambda_k}{4\pi^2}\displaystyle\sum_f |q_f B|\,\frac{|p_z|}{k}} . \quad (58)$$

We can then perform the momentum integration. For qualitative discussions we can treat $\lambda_k(\bar{p})$ with some typical $\bar{p}$ in Eq. (58).

In the vicinity of chiral phase transition, λ_k in $\lambda_k(p)$ becomes larger and larger as k decreases, which is a flow pattern implied from Eq. (45). Naïvely, one might have thought that the effect of the diagrams (b)–(d) is just to replace the overall factor in the β-function, but this is not the case once the momentum dependence in the running coupling constant is taken into account. As is clear from Eq. (58), we can see,

$$\lambda_k(\bar{p}) \to (\text{const.}) \qquad (\lambda_k \to \infty;\ k \to 0) . \quad (59)$$

This means that the contribution from the diagram (a) which is proportional to λ_k^2 overwhelms (b)–(d) which are proportional to $\lambda_k(\bar{p})\lambda_k$ and $\lambda_k(\bar{p})^2$, respectively, near the chiral phase transition. Therefore, our analysis of (a) in the previous section is not changed by the inclusion of (b)–(d) qualitatively.

To go into more quantitative studies, however, it is inadequate to use λ_k that is solved previously, but we need to solve the flow equation self-consistently including the non-local vertices.

B. Self-consistent resummation

Finally we advance our truncation scheme for taking account the non-local vertices $\lambda_k(p)$. The result for $\lambda_k(p)$ discussed previously stems from a standard resummation of bubble diagram in the s-channel or the leading-order contribution in the $1/N_{\rm c}$ expansion. Now we utilize the flow for going beyond this approximation. For that purpose we parameterize the full s-channel coupling $\lambda_k(p)$ as

$$\lambda_k(p) = \frac{\bar{\lambda}_k(p)}{1 - \bar{\lambda}_k(p)\Delta\Pi_k(p)} \quad (60)$$

with an unknown function $\bar{\lambda}_k(p)$. One can understand this Ansatz as a running coupling (56) with shifted renormalization. That is, one can immediately reach Eq. (60) by the following replacement in Eq. (56);

$$\frac{1}{\lambda_k} + \Delta\Pi_\Lambda(p) \to \frac{1}{\bar{\lambda}_k(p)} . \quad (61)$$

We note that we have to promote the right-hand side as a momentum-dependent quantity to take account of the full resummation including (b)–(d) in addition to (a). We can fix the normalization at vanishing momentum as

$$\bar{\lambda}_k(0) = \lambda_k(0) = \lambda_k . \quad (62)$$

The flow of $\lambda_k(p)$ is, in principle, given by the flow equation with diagrams having momentum insertion from the external legs. For the derivation of the flow of $\bar{\lambda}_k(p)$ we can take the derivative on Eq. (60) to find,

$$\frac{\partial_k \bar{\lambda}_k(p)}{\bar{\lambda}_k(p)} = \frac{\partial_k \lambda_k(p)}{\lambda_k(p)}\frac{1}{1 + \lambda_k(p)\Delta\Pi_k(p)} - \lambda_k(p)\partial_k\Delta\Pi_k(p) . \quad (63)$$

For the solution of the flow $\partial_k\bar{\lambda}_k(p)$ in Eq. (63) we have to insert the flow of $\partial_k\lambda_k(p)$ in a given approximation. A fully self-consistent flow results in loops with momentum-dependent four-point vertex which would require numerical computations of the Dyson-Schwinger type.

In the present work we invoke further approximations motivated by the physics under discussion. This also facilitates the task of solving the flows and to uncover the underlying mechanisms.

The coupling parameter $\bar{\lambda}_k(p)$ encodes the pion effects beyond the leading s-channel resummation. These effects, as is already the case in the previous subsection

for the s-channel resummation, are suppressed for non-zero internal momenta. This structure enables us to solve the flow for $\bar{\lambda}_k(p)$ within a derivative expansion in the s-channel momentum p. It also helps that the successive integration in terms of k already includes the momentum-dependence of $\bar{\lambda}_k(p)$ within the identification,

$$\lambda_{k=0}(q) \simeq \lambda_{k=q}(0) \ . \tag{64}$$

Equation (64) also provides a self-consistency check of the current derivative expansion. In the present work we take the lowest-order derivative expansion as $\bar{\lambda}_k(p) \simeq \bar{\lambda}_k(0) = \lambda_k$ [see Eq. (62)] and, analogously to the flow equation (23), we arrive at

$$\partial_k \lambda_k = \sum_{i=a,b,c,d} \mathrm{Diag}^{(i)} \ , \tag{65}$$

where $\mathrm{Diag}^{(i)}$ with $i = a, b, c, d$ stands for the momentum integrations corresponding to the diagrams (a)–(d). With the coupling $\lambda_k(p)$ put down in Eq. (60) the diagrams take the form;

$$\mathrm{Diag}^{(a)} = -8N_\mathrm{c} \sum_{f=u,d} \int \frac{\mathrm{d}^4 p}{(2\pi)^4} \, \lambda_k^2 \, I_k(p_4, \vec{p}) \ , \tag{66}$$

$$\mathrm{Diag}^{(b)} + \mathrm{Diag}^{(c)} = -4 \sum_{f=u,d} \int \frac{\mathrm{d}^4 p}{(2\pi)^4} \, \frac{\lambda_k^2}{1 - \lambda_k \Delta\Pi_k(p)} \, I_k(p_4, \vec{p}) \ , \tag{67}$$

$$\mathrm{Diag}^{(d)} = \sum_{f=u,d} \int \frac{\mathrm{d}^4 p}{(2\pi)^4} \, \frac{\lambda_k^2}{[1 - \lambda_k \Delta\Pi_k(p)]^2} \, I_k(p_4, \vec{p}) \ . \tag{68}$$

with the common integrand given by

$$I_k(p_4, \vec{p}) = \frac{\partial_k r_k(\vec{p}) \, \vec{p}^2 [1 + r_k(\vec{p})]}{\{p_4^2 + \vec{p}^2 [1 + r_k(\vec{p})]^2\}^2} \ . \tag{69}$$

For the diagram (a) the s-channel momentum is the external one for both couplings and hence λ_k^2 appears in the integration just in the same way as in Eq. (23). For the diagrams (b) and (c) one of two couplings has zero momentum in the s-channel and the other has the loop momentum p. Finally, for the diagram (d), we have p for both vertices.

It should be noted that we have neglected isospin symmetry breaking in the above expressions. In other words, we here introduced simplification by setting the electric charges of u-quarks and d-quarks to be equal; $q_u = q_d$. Without this, the polarization $\Pi_k(p)$ is dependent on which flavors of quarks each diagram involves and thus $\lambda_k(p)$ should be also flavor dependent. As a result, for example, the charged pion propagations are suppressed and the contributions from (b) and (c) are vanishing due to cancellation between the π^0 and σ processes. We could have discussed all these complexities here, but they are not the main subject of the present work. We are only interested in formulating the resummation procedure here and looking over qualitative effects on the flow. Though we have to leave from real electromagnetism for the moment, we shall stick to simplicity with $q_u = q_d$.

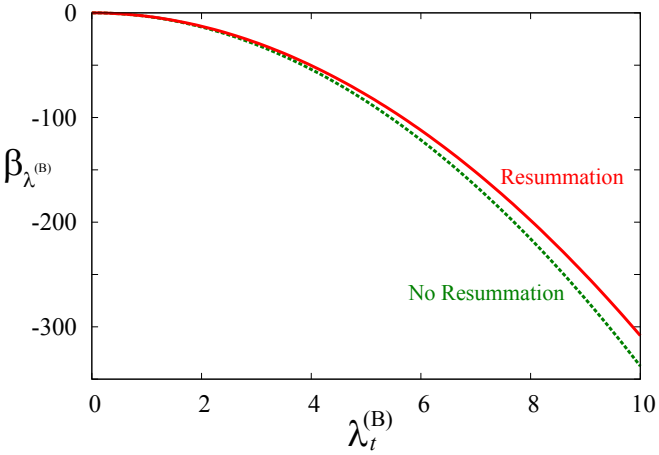

FIG. 4. Flow patterns of the four-Fermi coupling constant without resummation shown by the dotted line (in which the overall coefficient is $2N_\mathrm{c} + \frac{3}{4}$) and with resummation shown by the solid line.

Now we have a closed flow equation for λ_k. It takes into account the scale dependence of the coupling at vanishing momentum and goes beyond the standard bubble resummation. The current approximation fully restores RG-invariance; the coupling $\lambda_k(p)$ is invariant under a RG rescaling and looses all reference to the coupling at the cutoff, i.e., $\partial_{\lambda_\Lambda} \lambda_{k=0} = 0$.

Let us now discuss how the β-function is modified by this prescription of resummation. For this purpose we will again focus on the calculation in the strong $\boldsymbol{B}$ limit which enables us to use the LLLA for analytical calculations. In the LLLA, as we have seen, $\Delta\Pi_k(p)$ can be approximated as $\Delta\Pi_k(p) \simeq -(N_\mathrm{c}/4\pi^2) \sum_f |q_f B| (|p_z|/k)$. Since the momentum dependence is such simple, one can easily integrate each $\mathrm{Diag}^{(i)}$ with non-local vertices.

After the p_z-integration, with this resummation procedure, the β-function changes from Eq. (47) into

$$\partial_k \lambda_t^{(\mathrm{B})} = -N_\mathrm{c} \big(\lambda_k^{(\mathrm{B})}\big)^2 - \frac{\lambda_k^{(\mathrm{B})}}{N_\mathrm{c}} \ln\Big(1 + \tfrac{3}{2}\lambda_k^{(\mathrm{B})}\Big) + \frac{(\lambda_k^{(\mathrm{B})})^2}{8\big(1 + \frac{3}{2}\lambda_k^{(\mathrm{B})}\big)} \ . \tag{70}$$

The behavior of the right-hand side is shown in Fig. 4. We can see that the resummation has a minor effect as stated in qualitative discussions in the previous subsection. The resummation tends to disfavor chiral symmetry breaking slightly, which is consistent with the intuition that meson fluctuations would rather restore chiral symmetry.

V. CONCLUSION

We have investigated the RG flow pattern of the four-Fermi coupling constant λ_k and clarified the intuitive picture of the chiral phase transition at zero and finite temperature and baryon density. We have applied the formalism to study the effects of the homogeneous magnetic field. In the RG analysis it is extraordinarily simple to understand the phenomenon called the Magnetic Catalysis. If the magnetic field is strong enough, the transverse dynamics of charged particles is completely frozen and the dimensional reduction effectively occurs. Then, with the IR cutoff scale k, the transverse phase-space factor k^2 is replaced by the Landau degeneracy $|q_f B|/(2\pi)$, which changes the flow pattern significantly.

For dimensional reasons, in the absence of an external magnetic field $\boldsymbol{B}$, a dimensionless coupling constant is given by $\lambda_k k^2$, which tends to go to zero as k decreases unless the initial λ_Λ exceeds a critical value. In contrast, if strong magnetic fields $\boldsymbol{B}$ are applied, the dimensionless combination of coupling constant is rather characterized by $(\sum_f |q_f B|/2\pi^2)\lambda_k$. For this combination one can show that its RG flow leads to a diverging coupling however small the initial λ_Λ is. This is the simple RG-picture of the Magnetic Catalysis.

Our quantitative studies in numerical calculations have made it clear that the dimensional reduction, however, is a sensible approximation only when B is unrealistically large and the temperature T and the chemical potential $\mu_{\rm q}$ are sufficiently close to zero. The logarithmic singularity that is responsible for the Magnetic Catalysis is exactly canceled by another one from the matter parts at finite T and/or $\mu_{\rm q}$.

Finally, we have included the effects of non-local vertices mediated by the meson propagation with finite momentum. The resummation procedure argued in this work thus deals with separate contributions from meson loop effects and contains non-trivial contributions through the RG flow; see Ref. [40] for a similar kind of resummation. The related set of diagram has no qualitative impact on the location of the chiral phase transition. The present novel approximation to the NJL-model takes into account the back-reaction of intermediate mesonic states and hence relates to the full quark-meson flow in (P)QM models; see e.g. [12, 45–47]. We hence expect the present approximation to be sensitive to the critical properties of the phase transition. The discussion of critical properties is deferred to future extensions of the present work.

Although it was not quite necessary in the present work, it would be an intriguing question how to describe the neutral meson as charged quark composite in external $\boldsymbol{B}$. Our RG analysis clearly shows that the lowest Landau level approximation works for the neutral meson propagation only when B is greater than the cutoff scale Λ that roughly corresponds to the transverse meson size inverse. This means that the quark dissociation or deconfinement could be induced by the $\boldsymbol{B}$ effects, which would offer us a new opportunity to shed light on physics of quark confinement. Besides, it is an important but poorly understood problem to clarify the physical meaning of the conventional criterion for quark confinement using the Polyakov loop at strong $\boldsymbol{B}$, which would help us with understanding confinement/deconfinement at high density and hopefully more detailed characteristics of Quarkyonic Matter [48]. These are all interesting future extensions of the present work.

ACKNOWLEDGMENTS

The authors thank Jens Braun, Holger Gies, Kouji Kashiwa, Anton Rebhan, Andreas Schmitt for discussions.

[1] R. B. Laughlin, Phys. Rev. **B23**, 5632 (May 1981), http://link.aps.org/doi/10.1103/PhysRevB.23.5632
[2] D. E. Kharzeev, L. D. McLerran, and H. J. Warringa, Nucl. Phys. **A803**, 227 (2008), arXiv:0711.0950 [hep-ph]
[3] K. Fukushima, D. E. Kharzeev, and H. J. Warringa, Phys. Rev. **D78**, 074033 (2008), arXiv:0808.3382 [hep-ph]
[4] M. A. Metlitski and A. R. Zhitnitsky, Phys. Rev. **D72**, 045011 (2005), arXiv:hep-ph/0505072 [hep-ph]D. Kharzeev and A. Zhitnitsky, Nucl. Phys. **A797**, 67 (2007), arXiv:0706.1026 [hep-ph]D. E. Kharzeev and D. T. Son, Phys. Rev. Lett. **106**, 062301 (2011), arXiv:1010.0038 [hep-ph]
[5] T. Vachaspati, Phys. Lett. **B265**, 258 (1991)B.-l. Cheng and A. V. Olinto, Phys. Rev. **D50**, 2421 (1994)G. Baym, D. Bodeker, and L. D. McLerran, *ibid.* **D53**, 662 (1996), arXiv:hep-ph/9507429 [hep-ph]
[6] V. Gusynin, V. Miransky, and I. Shovkovy, Phys. Rev. Lett. **73**, 3499 (1994), arXiv:hep-ph/9405262 [hep-ph]Phys. Rev. **D52**, 4718 (1995), arXiv:hep-th/9407168 [hep-th]Phys. Lett. **B349**, 477 (1995), arXiv:hep-ph/9412257 [hep-ph]Nucl. Phys. **B462**, 249 (1996), arXiv:hep-ph/9509320 [hep-ph]
[7] V. Skokov, A. Illarionov, and V. Toneev, Int. J. Mod. Phys. **A24**, 5925 (2009), arXiv:0907.1396 [nucl-th]
[8] K. Tuchin, Phys. Rev. **C83**, 017901 (2011), arXiv:1008.1604 [nucl-th]K. Marasinghe and K. Tuchin, **C84**, 044908 (2011), arXiv:1103.1329 [hep-ph]
[9] U. W. Heinz, AIP Conf. Proc. **739**, 163 (2005), arXiv:nucl-th/0407067 [nucl-th]
[10] K. Fukushima, M. Ruggieri, and R. Gatto, Phys. Rev. **D81**, 114031 (2010), arXiv:1003.0047 [hep-ph]
[11] A. J. Mizher, M. Chernodub, and E. S. Fraga, Phys. Rev. **D82**, 105016 (2010), arXiv:1004.2712 [hep-ph]

[12] V. Skokov, Phys. Rev. **D85**, 034026 (2012), arXiv:1112.5137 [hep-ph]

[13] M. D'Elia, S. Mukherjee, and F. Sanfilippo, Phys. Rev. **D82**, 051501 (2010), arXiv:1005.5365 [hep-lat]

[14] G. Bali, F. Bruckmann, G. Endrodi, Z. Fodor, S. Katz, *et al.*, JHEP **1202**, 044 (2012), arXiv:1111.4956 [hep-lat]

[15] R. Gatto and M. Ruggieri, Phys. Rev. **D83**, 034016 (2011), arXiv:1012.1291 [hep-ph]

[16] K. Kashiwa, Phys. Rev. **D83**, 117901 (2011), arXiv:1104.5167 [hep-ph]

[17] B.-J. Schaefer, J. M. Pawlowski, and J. Wambach, Phys. Rev. **D76**, 074023 (2007), arXiv:0704.3234 [hep-ph]

[18] K. Fukushima, Phys. Lett. **B695**, 387 (2011), arXiv:1006.2596 [hep-ph]

[19] J. Braun, L. M. Haas, F. Marhauser, and J. M. Pawlowski, Phys. Rev. Lett. **106**, 022002 (2011), arXiv:0908.0008 [hep-ph]

[20] J. M. Pawlowski, AIP Conf.Proc. **1343**, 75 (2011), arXiv:1012.5075 [hep-ph]

[21] B. V. Galilo and S. N. Nedelko, Phys.Rev. **D84**, 094017 (2011), arXiv:1107.4737 [hep-ph]

[22] K. Fukushima, J. Phys. G **G39**, 013101 (2012), arXiv:1108.2939 [hep-ph]

[23] V. Gusynin, V. Miransky, and I. Shovkovy, Phys. Rev. **D52**, 4747 (1995), arXiv:hep-ph/9501304 [hep-ph]Phys. Rev. Lett. **83**, 1291 (1999), arXiv:hep-th/9811079 [hep-th]

[24] E. S. Fraga and A. J. Mizher, Phys. Rev. **D78**, 025016 (2008), arXiv:0804.1452 [hep-ph]

[25] H. Suganuma and T. Tatsumi, Annals Phys. **208**, 470 (1991)

[26] K. Fukushima and K. Kashiwa, work in progress

[27] F. Preis, A. Rebhan, and A. Schmitt, JHEP **1103**, 033 (2011), arXiv:1012.4785 [hep-th]

[28] D. K. Hong, Y. Kim, and S.-J. Sin, Phys. Rev. **D54**, 7879 (1996), arXiv:hep-th/9603157 [hep-th]

[29] D. D. Scherer and H. Gies(2012), arXiv:1201.3746 [cond-mat.str-el]

[30] J. Braun(2011), arXiv:1108.4449 [hep-ph]

[31] J. Berges(1998), arXiv:hep-ph/9902419 [hep-ph]

[32] K.-I. Kondo, Phys. Rev. **D82**, 065024 (2010), arXiv:1005.0314 [hep-th]

[33] T. Hatsuda and T. Kunihiro, Phys. Rept. **247**, 221 (1994), arXiv:hep-ph/9401310 [hep-ph]

[34] A. K. Das and M. B. Hott, Phys. Rev. **D53**, 2252 (1996), arXiv:hep-th/9504086 [hep-th]

[35] C. Wetterich, Phys. Lett. **B301**, 90 (1993)

[36] D. F. Litim and J. M. Pawlowski, World Sci., 168(1999), arXiv:hep-th/9901063 [hep-th]

[37] J. Berges, N. Tetradis, and C. Wetterich, Phys. Rept. **363**, 223 (2002), arXiv:hep-ph/0005122 [hep-ph]

[38] J. M. Pawlowski, Annals Phys. **322**, 2831 (2007), arXiv:hep-th/0512261 [hep-th]

[39] H. Gies(2006), arXiv:hep-ph/0611146 [hep-ph]

[40] J.-P. Blaizot, J. M. Pawlowski, and U. Reinosa, Phys. Lett. **B696**, 523 (2011), arXiv:1009.6048 [hep-ph]

[41] D. F. Litim and J. M. Pawlowski, JHEP **0611**, 026 (2006), arXiv:hep-th/0609122 [hep-th]

[42] D. F. Litim, Phys.Lett. **B486**, 92 (2000), arXiv:hep-th/0005245 [hep-th]

[43] L. Fister and J. M. Pawlowski(2011), arXiv:1112.5440 [hep-ph]

[44] K.-I. Aoki, K.-i. Morikawa, J.-I. Sumi, H. Terao, and M. Tomoyose, Prog. Theor. Phys. **97**, 479 (1997), arXiv:hep-ph/9612459 [hep-ph]

[45] V. Skokov, B. Stokic, B. Friman, and K. Redlich, Phys.Rev. **C82**, 015206 (2010), arXiv:1004.2665 [hep-ph]

[46] T. K. Herbst, J. M. Pawlowski, and B.-J. Schaefer, Phys.Lett. **B696**, 58 (2011), arXiv:1008.0081 [hep-ph]

[47] T. K. Herbst, J. M. Pawlowski, and B.-J. Schaefer(2012), arXiv:1202.0758 [hep-ph]

[48] L. McLerran and R. D. Pisarski, Nucl. Phys. **A796**, 83 (2007), arXiv:0706.2191 [hep-ph]